

Distinctive patterns on CT angiography characterize acute internal carotid artery occlusion subtypes

Ji Man Hong, MD, PhD^{a,*}, Sung Eun Lee, MD^a, Seong-Joon Lee, MD^a, Jin Soo Lee, MD, PhD^a, Andrew M. Demchuk, MD^b

Abstract

Noninvasive computed tomography angiography (CTA) is widely used in acute ischemic stroke, even for diagnosing various internal carotid artery (ICA) occlusion sites, which often need cerebral digital subtraction angiography (DSA) confirmation. We evaluated whether clinical outcomes vary depending on the DSA-based occlusion sites and explored correlating features on baseline CTA that predict DSA-based occlusion site.

We analyzed consecutive patients with acute ICA occlusion who underwent DSA and CTA. Occlusion site was classified into cervical, cavernous, petrous, and carotid terminus segments by DSA confirmation. Clinical and radiological features associated with poor outcome at 3 months (3–6 of modified Rankin scale) were analyzed. Baseline CTA findings were categorized according to carotid occlusive shape (stump, spearhead, and streak), presence of cervical calcification, Willisian occlusive patterns (T-type, L-type, and I-type), and status of leptomeningeal collaterals (LMC).

We identified 49 patients with occlusions in the cervical ($n = 17$), cavernous ($n = 22$), and carotid terminus ($n = 10$) portions: initial NIH Stroke Scale (11.4 ± 4.2 vs 16.1 ± 3.7 vs 18.2 ± 5.1 ; $P < 0.001$), stroke volume (27.9 ± 29.6 vs 127.4 ± 112.6 vs 260.3 ± 151.8 mL; $P < 0.001$), and poor outcome (23.5 vs 77.3 vs 90.0% ; $P < 0.001$). Cervical portion occlusion was characterized as rounded stump (82.4%) with calcification (52.9%) and fair LMC (94.1%); cavernous as spearhead occlusion (68.2%) with fair LMC (86.3%) and no calcification (95.5%); and terminus as streak-like occlusive pattern (60.0%) with poor LMC (60.0%), and no calcification (100%) on CTA.

Our study indicates that acute ICA occlusion can be subtyped into cervical, cavernous, and terminus. Distinctive findings on initial CTA can help differentiate ICA-occlusion subtypes with specific characteristics.

Abbreviations: CE = cardioembolism, CTA = computed tomography angiography, DSA = digital subtraction angiography, DWI = diffusion weight image, HT = hemorrhagic transformation, IA = intra-arterial, ICA = internal carotid artery, ICH = intracerebral hemorrhage, IV = intravenous, LMC = leptomeningeal collaterals, MCA = middle cerebral artery, mRS = modified Rankin scale, NIHSS = National Institutes of Health Stroke Scale, ROC = receiver operating characteristics, TICl = thrombolysis in cerebral ischemia, tPA = tissue plasminogen activator.

Keywords: acute, angiography, carotid artery, cerebral blood flow, cerebral hemodynamics, stroke subtype

1. Introduction

Sudden occlusion of the internal carotid artery (ICA) is usually associated with poor prognosis.^[1–4] Successful recanalization and good outcome in distal or terminal ICA occlusions have been

reported to be relatively low even after routine administration of intravenous (IV) tissue plasminogen activator (tPA).^[3,5] Recent clinical trials of endovascular treatment are making a noticeable change on the natural outcomes of patients presenting with proximal anterior circulation (ICA or middle cerebral artery [MCA]) acute ischemic stroke.^[6–10] Acute brain computed tomography (CT) or CT angiography (CTA) for prompt vascular assessment was a key element for such successful endovascular stroke trials.^[6,7] A variability in the clinical manifestations and prognosis of acute ICA occlusion can be explained by nature of its behaviors according to specific occlusion sites.^[11–13]

Determining the actual ICA occlusion sites with CTA is practical in clinical settings, as such noninvasive techniques can be done rapidly with minimal negative consequences. However, the findings can be misleading because CTA relies on a given vessel's blood flow stream during a particular scanning time.^[14,15] Due to stagnation or lack of flow in the upstream vessel, distal occlusions can manifest as proximal occlusions.^[14,15] In this study, we evaluated whether stroke severity and clinical outcome vary depending on the digital subtraction angiography (DSA) occlusion sites, and we investigated the correlation of various findings on CTA and DSA occlusion site by retrospective review of ICA occlusion patients from a prospectively-registered thrombolysis database in order to evaluate discrepancies between 2 angiographic modalities.

Editor: Massimo Tusconi.

JMH: make concepts, administrative support, data analysis, and manuscript writing; SEL, S-JL, JSL, and AMD: editing and data analysis.

The authors have no funding and conflicts of interest to disclose.

^a Department of Neurology, School of Medicine, Ajou University, Suwon, South Korea, ^b Calgary Stroke Program, Department of Clinical Neurosciences and Radiology, Hotchkiss Brain Institute, University of Calgary, Calgary, Alberta, Canada.

* Correspondence: Ji Man Hong, Department of Neurology, School of Medicine, Ajou University, 5 San, Woncheon-dong, Yongtong-gu, Suwon-si, Kyunggi-do 442-749, South Korea (e-mail: dacda@hanmail.net).

Copyright © 2017 the Author(s). Published by Wolters Kluwer Health, Inc. This is an open access article distributed under the Creative Commons Attribution-NoDerivatives License 4.0, which allows for redistribution, commercial and non-commercial, as long as it is passed along unchanged and in whole, with credit to the author.

Medicine (2017) 96:5(e5722)

Received: 25 August 2016 / Received in final form: 11 November 2016 /

Accepted: 28 November 2016

<http://dx.doi.org/10.1097/MD.0000000000005722>

2. Methods

2.1. Study population

We retrospectively reviewed clinical demographics, and radiological findings in ischemic stroke patients registered in a prospective digitalized endovascular database in a single referral stroke center composed of mainly Asian ethnic group from March 2006 to April 2009. We excluded the patients who were admitted after introduction of stent retrieval devices. Eligibility criteria were an intention to perform endovascular therapies due to occlusion of the proximal cerebral vessel documented on CTA, symptoms and signs of an anterior circulation stroke on admission, National Institutes of Health Stroke Scale (NIHSS) score ≥ 5 , and symptomatic ICA occlusion on DSA. We excluded patients when ischemic stroke involved only the posterior circulation, isolated anterior cerebral artery, or isolated MCA, when the patient had no large-vessel occlusion despite an apparent diffusion weight image (DWI) lesion, and when other determined etiologies (i.e., carotid dissection) were suspected. All included patients underwent diagnostic studies including routine blood tests and cardiologic work-ups. A detailed profile for the study population is shown in Fig. 1.

2.2. Protocol for acute stroke patients

Baseline CT scans (including nonenhanced and enhanced axial parenchymal images) and CTA were immediately obtained at the emergency room if acute stroke was suspected. The CTA was reconstructed with maximal intensity projection and volume-rendering techniques. IV-tPA was administered (0.9 mg/kg) in patients within 3 h of onset. Patients without contraindications for endovascular treatment underwent the intra-arterial (IA) approach as soon as possible if the onset-to-decision interval was < 5 h.^[16] Combined IV and IA thrombolysis was also performed if necessary. Recanalization status was determined by

neuro-interventionists on final angiography. Immediately after the endovascular procedure was completed, a nonenhanced CT was obtained. Magnetic resonance imaging consisting of axial T2-weighted, DWI, and gradient echo T2-weighted images was performed within 1 day of admission. This study was approved by the Institutional Review Board of Ajou University Hospital and it conformed to the provisions of the Declaration of Helsinki. Consent forms were waived due to the retrospective design.

2.3. Acquisition of Images

The stroke CT protocol using a multi-detector CT scanner (Sensation 16, Siemens, Erlangen, Germany) included non-enhanced, angiographic, and enhanced head CT scans from the vertex to aortic arch by use of the axial technique. Nonenhanced CT with 5-mm thick slices was followed by CTA using 1-mm thick sections. A volume of 100 mL of 68% nonionic contrast dye was administered with a power injector into the antecubital vein at a rate of 4 to 5 mL/s before CTA acquisition. CTA scanning began when enhancement in the common carotid arteries reached 120 Hounsfield units. Reconstruction of raw data from the CTA was achieved using a soft-tissue algorithm with a section thickness of 1.5 and 1.0 mm reconstruction intervals. The CTA source images were postprocessed to create coronal, sagittal, and axial multiplanar reformats in maximum intensity projection images and volume rendered 3D images.

A guiding catheter with Envoy (Cordis, Miami, FL) or Shuttle (Cook, Cook, IN) was used to select the ICA via a transfemoral approach. The ICA occlusion sites were designated as the location with contrast media arrest of the ICA until the maximally delayed venous phase. Bilateral ICAs and vertebral arteries were examined. The angiographic recanalization status was evaluated by the thrombolysis in cerebral ischemia (TICI) system.^[17] A TICI score of 2b to 3 was considered to indicate successful recanalization.

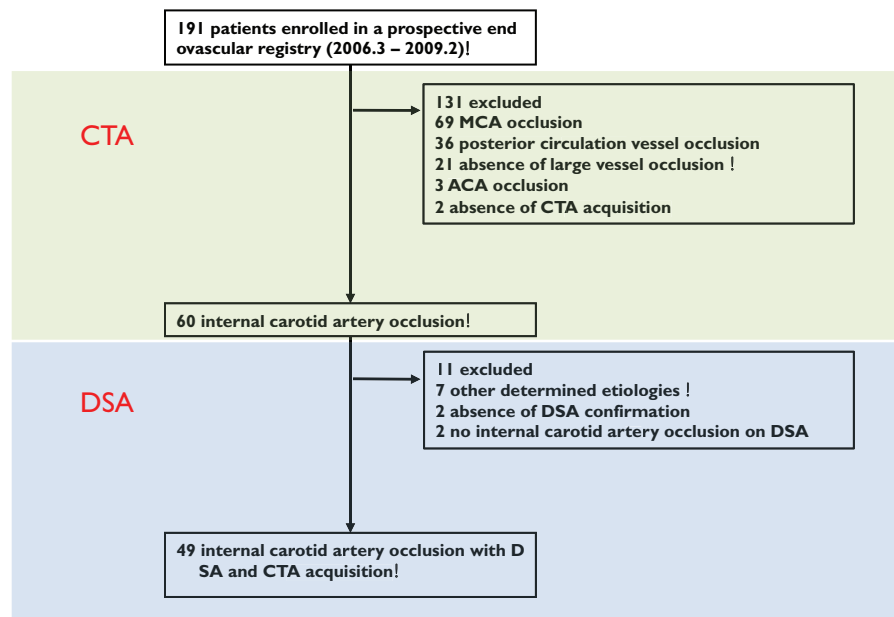


Figure 1. A flow diagram of the enrolled patients. A total of 191 consecutive patients with acute ischemic stroke from a prospective digitalized thrombolysis database over 3 years. ACA=anterior cerebral artery, CTA=computed tomography angiography, DSA=digital subtraction angiography, MCA=middle cerebral artery.

2.4. Analysis of Images

Two neurologists (JMH and JSL) reviewed the images including the CT, magnetic resonance imaging, and angiography scans through consensus in an adjudication meeting. Occlusive patterns and characteristics on baseline CTA with maximum intensity projection images and 3D reconstructions are shown in Fig. 2. Carotid occlusive patterns were categorized into 3 types by CTA: stump, spearhead, and streak or elongation.^[18] The presence of carotid calcification was determined as any lesion area of at least $\geq 1 \text{ mm}^2$ with attenuation >500 Hounsfield units.^[19] Occlusive patterns of the circle of Willis on baseline CTA were categorized into T-type, L-type, and I-type (patent type) according to a previous study.^[20] The status of leptomeningeal collaterals (LMC) was regarded as “poor” if no or minimal collaterals in a region $>50\%$ within the MCA territory when compared to pial filling on the contralateral side; and “fair or good” if similar or more collaterals within the MCA territory on maximum intensity projection images before the venous phase. The designation of the ICA occlusion site was confirmed by DSA, regardless of other tandem occlusive lesions. The ICA segments were divided into 4 parts by DSA: cervical, petrous, cavernous, and terminus or supraclinoid segments according to Gibo’s classification.^[21] On a 48-h noncontrast CT scan, hemorrhagic transformation (HT) was classified into 4 subtypes: HT type 1 and 2, and parenchymal hemorrhage type 1 and 2.^[22] Symptomatic intracranial hemorrhage was defined as ≥ 4 -point increase in the NIHSS score. Infarct volume was measured on the DWIs ($b=1000 \text{ s/mm}^2$). Whenever ≥ 1 lesion was present, the additional lesions were manually contoured. The volume was obtained by multiplying every contoured lesion by the slice thickness plus the intersection gap.

2.5. Short-term prognosis and stroke mechanisms

All patients were evaluated with the NIHSS score on days 1, 3, 7 after admission, and at discharge, and the modified Rankin scale (mRS) at 90 days via face-to-face or telephone interview. The clinical outcome was dichotomized into good (mRS 0–2) and poor (mRS 3–6) at 90 days after admission. To classify the stroke

etiology, we categorized all cases into 3 groups: cardioembolism (CE), large-artery atherosclerosis, and combined.^[23]

2.6. Statistical analysis

Differences between groups were analyzed using analysis of variance and the chi-squared test, for continuous and categorical variables. The values were considered via the nonparametric tests among the groups when the data were not normally distributed. Potential predictors of poor outcome (mRS 3–6) were entered into a univariate logistic regression model—general demographics: age, sex, onset to CT time; stroke severity: NIHSS at baseline and stroke volume on DWI; occlusion sites: cervical, cavernous, and terminus segments; stroke mechanism: atherosclerosis, CE, and combined; thrombolysis modality: IV thrombolysis only, IA thrombolysis only, and IV–IA combined; successful recanalization; and symptomatic ICH. Potentially significant predictors ($P < 0.1$) in the univariate analysis were included in the final multivariate model. A stepwise backward conditional method was performed in the final multivariate model. We described receiver operating characteristic (ROC) curves to predict the DSA-confirmed ICA occlusion site (cervical, cavernous, or terminus occlusion) with baseline findings on CTA (carotid occlusive patterns [stump, spearhead, streak, or elongation], presence of cervical calcification, Willisian occlusive patterns [T-type, L-type, and I-type], and status of LMC). We also described ROC curves to discriminate the DSA-confirmed ICA occlusion sites, respectively, using a composite score of 4-specific items representing carotid and Willisian occlusive patterns. Statistical analyses were performed using commercially available software (SPSS, version 18.0). P values < 0.05 were considered significant.

3. Results

3.1. Clinical characteristics and patient outcome

Among 191 consecutive patients who underwent endovascular approach during the study period in a prospective endovascular registry, a total of 49 strokes patients were attributed to ICA

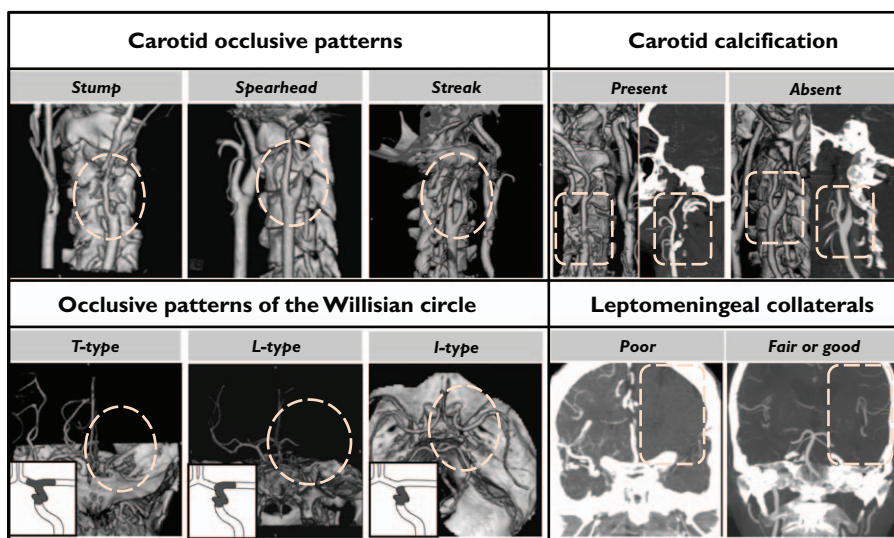


Figure 2. Dotted circles and squares indicate 4 characteristic findings on initial computed tomography angiography: carotid occlusive patterns (stump, spearhead, and streak), presence of cervical calcification, occlusive patterns of the Willisian circle (T-type, L-type, and I-type), and status of leptomeningeal collaterals (poor and fair or good).

occlusion with confirmation by DSA and CTA. The mean age was 67 ± 12 years, median NIHSS score 15, and onset-to-CT time 79 min. Twenty-three patients (46.9%) were successfully recanalized (TICI 2b or 3) in this study.

Details of the clinical features of the study population according to DSA occlusion site subtypes are shown in Table 1. Occlusion sites on DSA were as follows: cervical occlusion ($n = 17$, 35%), cavernous occlusion ($n = 22$, 45%), and terminus occlusion ($n = 10$, 20%). Occlusion was not found in the petrous segment. Age and gender did not vary according to the ICA occlusion site. Initial stroke severity differed between cervical, cavernous and terminal occlusions (11.4 ± 4.2 vs 16.1 ± 3.7 vs 18.2 ± 5.1 , $P < 0.001$; stroke volume: 27.9 ± 29.6 vs 127.4 ± 112.6 vs 260.3 ± 151.8 mL, $P < 0.001$). The neurological severity and stroke volume increased with more distal involvement. Embolic mechanisms were more frequent with distal occlusions (11.8% vs 50.0% vs 80.0%, $P = 0.003$).

Symptomatic ICH (5.9% vs 40.9% vs 60%, $P = 0.008$) was more prevalent in distal occlusions, including cavernous and terminus portions. In addition, radiological HT pattern of the cerebral parenchyma ($P < 0.001$), mortality rate (0.0% vs 36.4% vs 60%, $P = 0.002$), and outcome of 3-month mRS 3 to 6 (23.5% vs 77.3% vs 90.0%, $P < 0.001$) were significantly different amongst the groups. Recanalization rates (58.8% vs 40.9% vs 50.0%, $P = 0.593$) and onset-to-CT time (112 vs 110 vs 78 min, $P = 0.418$) were not significantly different among the groups.

Table 1
Clinical characteristics of the study population according to the DSA-confirmed ICA occlusion sites.

	Cervical (n=17)	Cavernous (n=22)	Terminus (n=10)	P
General demographics				
Age, y	69.1 ± 10.8	65.5 ± 11.6	70.2 ± 12.5	0.485
Male, n (%)	15 (88.2)	15 (68.2)	5 (50.0)	0.095
Onset to CT time, min	112 ± 68	110 ± 76	78 ± 55	0.418
Median NIHSS at baseline, IQR	11.4 ± 4.2	16.1 ± 3.7	18.2 ± 5.1	<0.001
Lesion volume on DWI, mL	27.9 ± 29.6	127.4 ± 112.6	260.3 ± 151.8	<0.001
Stroke mechanisms, n (%)				0.003
Atherosclerosis	14 (82.4)	7 (31.8)	2 (20.0)	
Cardioembolism	2 (11.8)	12 (54.5)	8 (80.0)	
>1 cause	1 (5.9)	3 (13.6)	0 (0)	
Thrombolysis, n (%)				0.057
IV-tPA only	12 (70.6)	6 (27.3)	4 (40.0)	
IA only	3 (17.7)	6 (27.3)	1 (10.0)	
IV-IA combined	2 (11.8)	10 (27.3)	5 (50.0)	
Successful recanalization, %	7 (41.1)	11 (50.0)	5 (50.0)	0.841
Neurologic complications, n (%)				
HT				<0.001
None	7 (41.2)	3 (13.6)	0 (0.0)	
HT1	7 (41.2)	4 (18.2)	1 (10.0)	
HT2	1 (5.9)	3 (13.6)	1 (10.0)	
PH1	2 (11.8)	5 (22.7)	2 (20.0)	
PH2	0 (0.0)	7 (31.8)	6 (60.0)	
Symptomatic ICH	1 (5.9)	9 (40.9)	6 (60.0)	0.008
Outcome, n (%)				
Mortality within 3 mo	0 (0.0)	8 (36.4)	6 (60.0)	0.002
3–6 of mRS at 3 mo	4 (23.5)	17 (77.3)	9 (90.0)	<0.001

11 (8.5–13.5) versus 16 (14–18) versus 18 (15.5–20.5); $P < 0.001$.

CT = computed tomography, DSA = digital subtraction angiography, DWI = diffusion weight image, HT = hemorrhagic transformation, IA = intra-arterial, ICA = internal carotid artery, ICH = intracerebral hemorrhage, IQR = interquartile range, IV = intravenous, mRS = modified Rankin scale, NIHSS = National Institutes of Health Stroke Scale, PH = parenchymal hemorrhage, tPA = tissue plasminogen activator.

3.2. Characteristic CTA patterns according to DSA occlusion subtypes

Baseline CTA findings according to DSA occlusion subtypes are shown in Table 2. Carotid occlusive patterns were significantly different ($P < 0.001$): the stump (82.4%) was the most common pattern in cervical occlusion, the spearhead (68.2%) was the most common in cavernous occlusion, and streak pattern (60.0%) was the most prominent in terminus occlusion. The prevalence of carotid calcification was significantly higher in cervical occlusion (52.9% vs 4.5% vs 0.0%, $P < 0.001$).

Willisian occlusive patterns according to the DSA occlusion subtype were also significantly different ($P = 0.049$); a higher proportion of T-type was observed in terminus occlusion (80.0%) and cavernous occlusion (59.1%), whereas the patency pattern was the most common in cervical occlusion (58.9%). Moreover, a difference in the status of LMC was detected according to subtype; poor collaterals were significantly frequent with increasing trend toward distal occlusions (5.9% vs 13.6% vs 60.0%, $P = 0.011$).

3.3. Discrimination of DSA occlusion sites by baseline CTA

Figure 3A shows the prevalent characteristic CTA patterns according to ICA occlusion sites outlined in Table 2 through bar graphs. Figure 3B shows the area under the ROC curves to discriminate sensitivity and specificity for the DSA occlusion site based on 4 specific findings: cervical carotid occlusive patterns, presence of cervical calcification; Willisian occlusive patterns, and status of LMC. The area under the ROC curve for cervical ICA occlusion was highest at 0.910 with a composite score of 4 items: stump (area, 0.771), presence of calcification (area, 0.733), Willisian patency (area, 0.700), and good collaterals (area, 0.596). The area under the ROC curve for the cavernous ICA occlusion was also the highest at 0.825 with a composite score of following items: spearhead (area, 0.771), no calcification (area, 0.662), Willisian patency (area, 0.555), and good collaterals (area, 0.543). The area under the ROC curve for the terminus occlusion was highest at 0.849 with a composite score of

Table 2
Characteristic CTA patterns according to the DSA-confirmed ICA occlusion sites.

	Cervical (n=17)	Cavernous (n=22)	Terminus (n=10)	P
Carotid occlusive patterns				
Stump	14 (82.4)	4 (18.2)	3 (30.0)	<0.001
Spearhead	0 (0.0)	15 (68.2)	1 (10.0)	
Streak	3 (17.6)	3 (13.6)	6 (60.0)	
Carotid calcification				
Present	9 (52.9)	1 (4.5)	0 (0.0)	<0.001
Absent	8 (47.1)	21 (95.5)	10 (100.0)	
Willisian occlusive patterns				
T-type	5 (29.4)	13 (59.1)	8 (80.0)	0.049
L-type	2 (11.8)	4 (18.2)	1 (10.0)	
I-type	10 (58.9)	5 (22.7)	1 (10.0)	
Leptomeningeal collateral status				
Poor	1 (5.9)	3 (13.6)	6 (60.0)	0.011
Fair or good	16 (94.1)	19 (86.3)	4 (40.0)	

CTA = computed tomography angiography, DSA = digital subtraction angiography, ICA = internal carotid artery.

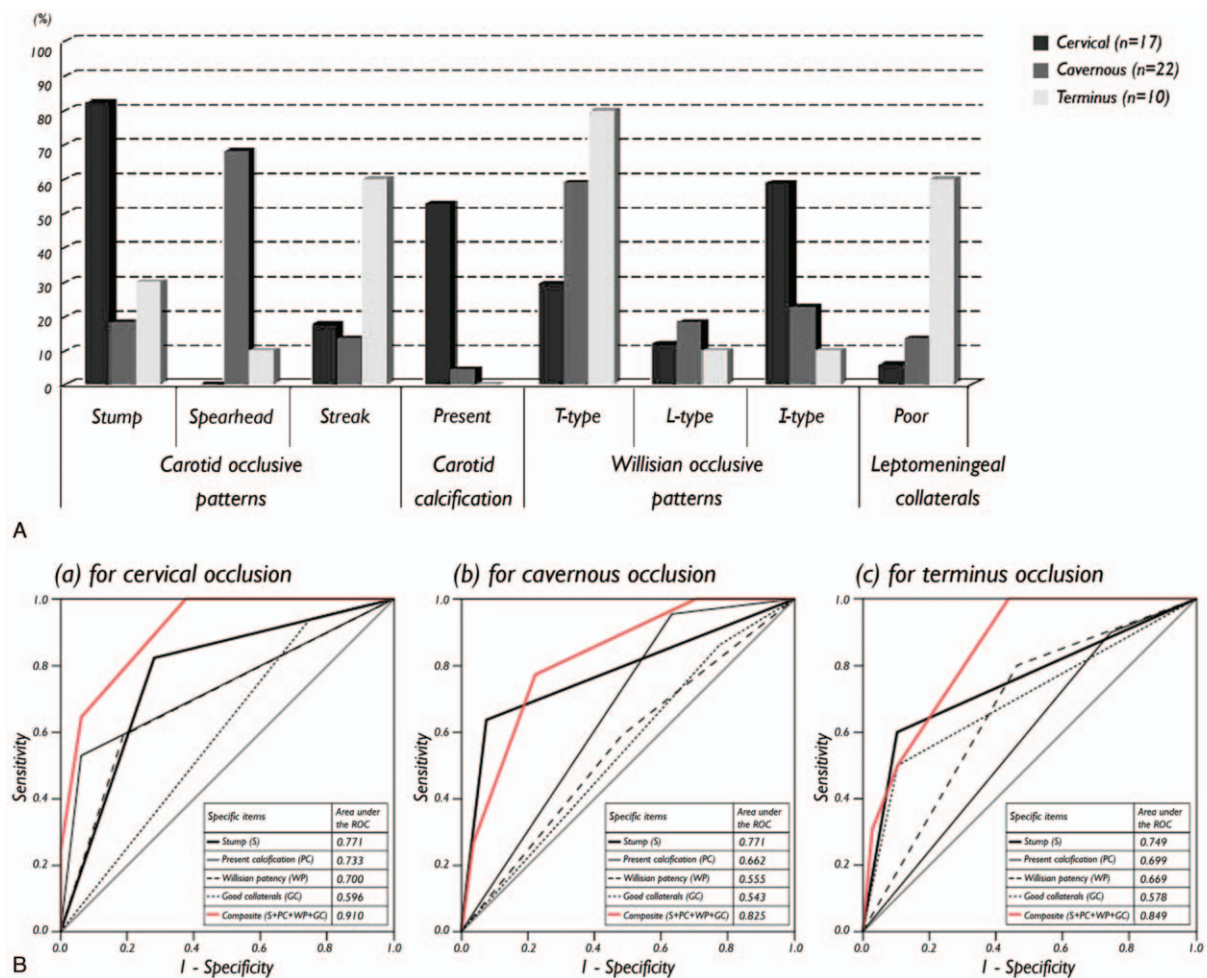


Figure 3. (A) The frequency of characteristic patterns (carotid occlusive patterns, presence of carotid calcification, occlusive patterns of the Willisian circle, and status of leptomeningeal collaterals) on initial CTA according to the DSA-confirmed ICA occlusion site. CTA shows distinctive characteristics according to the DSA-confirmed ICA occlusion sites. (B) ROC curves using the characteristic patterns on initial CTA to differentiate the actual DSA occlusion sites. Composite scores of 4 characteristic patterns show the highest areas in the ROC curves for pinpointing the ICA occlusion site: (a) cervical portion, (b) cavernous portion, and (c) terminus portion. CTA=computed tomography angiography, DSA = digital subtraction angiography, ICA=internal carotid artery, ROC=receiver operating characteristic.

following items: Willisian patency (area, 0.749), poor collateral (area, 0.699), T-type occlusion (area, 0.669), and absent calcification (area, 0.578).

3.4. Multiple regression analysis for predicting short-term outcome

To evaluate independent predictors of poor prognosis (mRS 3–6 at 90 days), potential factors were entered into a univariate analysis with poor outcome as a dependent variable. Age, gender, baseline NIHSS, initial stroke volume, occlusion site, stroke mechanism, and symptomatic ICH remained significant predictors of poor outcome. After adjusting for those variables in a multiple logistic regression analysis, age (odds ratio, 1.1 per 1-year increase; 95% confidence interval, 1.0–1.2, $P=0.045$) and distal involvement (cavernous and terminus) (odds ratio, 10.0; 95% confidence interval, 1.4–74.4, $P=0.024$) remained as independent factors for poor outcome. Gender, baseline NIHSS, stroke volume, CE, and symptomatic ICH did not remain in the final model (Table 3).

4. Discussion

Our findings show that patients with acute ICA occlusions can be separated into 3 distinct subtypes according to the DSA-confirmed ICA occlusion sites: cervical, cavernous, and terminus. These categories can be clearly differentiated through clinical variables and outcomes, and they can be easily identified on initial CTA in the present study.

4.1. DSA occlusion subtypes: clinical and radiological variability

Previous studies have reported that patients with ICA occlusion have various clinical manifestations (i.e., monocular blindness, hemiparesis, hemiplegia, cortical symptoms, and coma) and diverse severity (i.e., transient ischemic attack to a massive herniated form of territorial infarction).^[11,24] Our study shows that the clinical variability in ICA occlusions is significantly associated with the DSA-confirmed ICA occlusion site. The leading cause of ICA terminus occlusion has been associated with severe stroke symptoms by CE and the etiology of primary

Table 3**Multivariate regression analysis on baseline variables to predict poor outcome (mRS 3–6 at 90 d).**

	Good (n = 19)	Poor (n = 30)	P	Crude OR (95% CI)	P	Adjusted OR (95% CI)	P
General demographics							
Age, y	64.3 (11.5)	69.9 (11.1)	0.094	1.05 (0.99–1.10)	0.098	1.10 (1.00–1.20)	0.045
Female, n (%)	2 (10.5)	12 (40.0)	0.026	5.67 (1.10–29.13)	0.038	—	—
Onset to CT time, min	102 (56)	107 (78)	0.823	1.00 (0.99–1.01)	0.818		
Stroke severity							
Baseline NIHSS	12.1 (4.2)	16.6 (4.6)	0.001	1.30 (1.09–1.55)	0.004	—	—
Stroke volume on DWI, mL	34 (57)	175 (136)	0.000	1.02 (1.01–1.04)	0.005	—	—
Occlusion sites							
Cervical	13	4		Reference			
Distal (above cavernous)	6	26		14.08 (3.37–58.83)	<0.001	10.03 (1.35–74.35)	0.024
Stroke mechanisms, n (%)							
Atherosclerosis	14	9	0.005	Reference			
Cardioembolism	3	19		9.85 (2.24–43.18)	0.002	—	—
>1 cause	2	2		1.56 (0.186–13.11)	0.685		
Thrombolysis, n (%)							
IV-tPA only	13	9	0.022	Reference			
IA only	1	8		0.64 (0.08–5.42)	0.685		
IV–IA combined	5	13		6.33 (0.63–63.64)	0.117		
Successful recanalization, %	10 (52.6)	13 (43.3)	0.526	0.68 (0.21–2.18)	0.526		
Symptomatic ICH	2 (10.5)	14 (46.7)	0.009	7.44 (1.46–38.01)	0.016	—	—

CI = confidence interval, CT = computed tomography, DWI = diffusion weight image, IA = intra-arterial, ICH = intracerebral hemorrhage, IV = intravenous, mRS = modified Rankin scale, NIHSS = National Institutes of Health Stroke Scale, OR = odds ratio, tPA = tissue plasminogen activator.

cervical ICA occlusion has been related to mild stroke symptoms including transient ischemic attacks and hemodynamic stroke by “atherosclerosis” in the acute and chronic phases.^[25,26] In this study, stroke mechanisms were also consistent with these common findings in patients with respective cervical or distal ICA occlusion.

Few studies have focused on differentiating these separate stroke subtypes in acute ICA occlusion, while many have emphasized treatment options suitable only in proximal cervical occlusions.^[4,6] Our findings appear to support the concept of acute cervical occlusion and its association with good outcome which is implied by higher rates of Willisian patency (I-type) and good collaterals. Moreover, our data show that distal ICA occlusion is associated with poor outcome, likely because of the lack of cerebral collaterals from complete occlusion at the ICA terminus. Therefore, the variability of clinical severity and outcomes in acute ICA occlusion may be explained by the ultimate cerebral blood flow of ischemic tissue, the burden of the thrombus, and the compensatory perfusion state from various collaterals.^[11,27]

Despite actual distal ICA occlusion at the cavernous or terminus portion on DSA, patients with stump or spearhead carotid occlusive pattern (25/34, 73%) on baseline CTA can be misleadingly interpreted as proximal ICA occlusion (Table 2). In order to predict the actual ICA occlusion site, thus, we suggest that the initial CTA findings be carefully categorized by the following patterns: carotid occlusive patterns, presence of cervical calcification, Willisian occlusive patterns, and status of LMC. These 4 specific characteristics on the initial CTA can help identify the actual ICA occlusion subtypes without invasive DSA.

4.2. Clinical significance of initial CTA findings in discriminating ICA occlusion subtypes

Using noninvasive CTA, rapid pinpointing of the occlusion is important as the treatment options vary with the mechanism of ischemia.^[11,12] Because noninvasive image acquisition is based on its blood flow stream in the vessel during a given exposure

time, images are obtained when there is flow momentum.^[28] When acute occlusion occurs in the ICA without the presence of daughter vessels, blood flow may be congested at the proximal portion of the ICA, regardless of the true occlusion site.^[14,15] In acute stroke patients with proximal artery occlusions, IV-tPA alone appears to have somewhat lower reperfusion rates and poor outcomes.^[5] Early recognition of the distal occlusion of the ICA using characteristic composite items on initial CTA can be a powerful ally for the clinician when collaborated with state-of-the-art stent retrieval system.^[29]

4.3. Hemodynamic mechanisms for “pretreatment CTA findings”

Our findings indicate that the terminal ICA portion group tends to have more “T-type occlusions” without LMC compared with other groups. When the cases are completely occluded by a clot of the blood around the terminal or cavernous ICA, arterial flow cannot be easily generated because of its specific anatomy of a “relatively rigid pipe without an offshoot” (i.e., a long and stiff tube with long bony sheath and no branches until the ophthalmic artery).^[19] Therefore, the “spearhead and streak” formation on an angiographic image can be reflective of stagnation of blood flow at the cervical ICA portion in cases with the cavernous and terminus ICA occlusion (Fig. 3B).

In this study, a rounded-stump pattern of the carotid represented an occlusion in the cervical portion of the ICA (60.9%). The cessation of flow in proximity to the carotid bifurcation causes this appearance (Fig. 4). In the case of an acute cervical ICA occlusion, this type of stump can be shown, as separated flow after bifurcation lack enough entry length for sufficient flow momentum in the ICA tube.^[28] Compared to other occlusion sites (3%), our study showed that there was a higher presence of vascular calcification (53%) in cervical ICA occlusions. Previous studies revealed that vascular calcification is a typical surrogate maker of atherosclerosis in patients with major vessel disease and our data also support this concept.^[30]

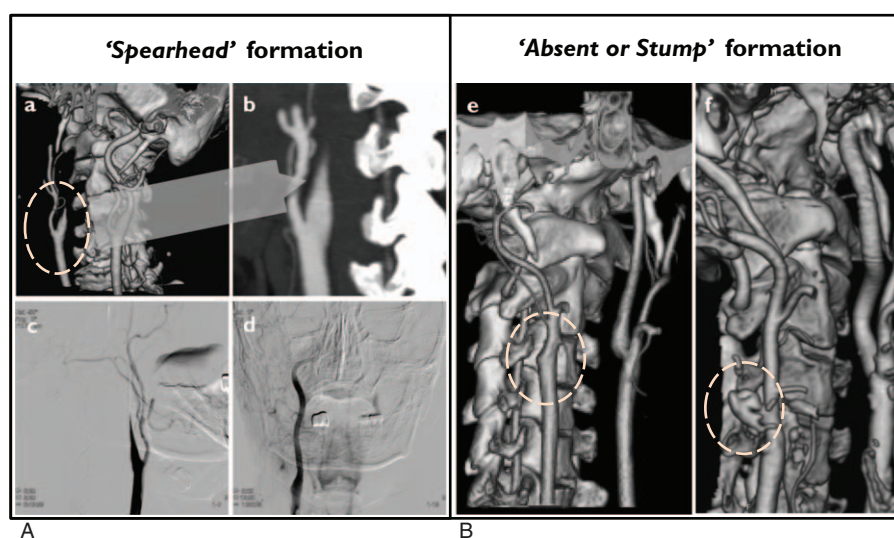


Figure 4. "Spearhead" formation (A) and "absent or stump" formation (B) in patients with ICA occlusion. "Spearhead" is shown in 3D-reconstruction (a) and MIP (b) images on initial CTA. Its trajectory on DSA is observed approximately 30% longer in the same patient during handed injection with iodine contrast at the level of the common carotid artery than the trajectory on CTA (c). The cavernous portion on DSA is the actual occlusion site in this patient (d), although initial CTA occlusion indicates the cervical portion. (B) Three-dimensional reconstruction CTA shows absence (e) and rounded stump (f) of the occluded ICA with calcification (dotted circle). 3D=3-dimensional, CTA=computed tomography angiography, DSA = digital subtraction angiography, ICA=internal carotid artery, MIP=maximum intensity projection.

4.4. Limitations

We acknowledge some limitations in this study. First, it is comprised of relatively small sample size and is subject to the biases of a single center observational study. However, we tried to overcome this limitation by including patients in a given period of time who received coherent IV and/or endovascular thrombolysis. Our observation is also somewhat hypothetical because we addressed the anatomical properties and morphological features according to ICA occlusion sites. Moreover, our results should be cautiously interpreted because IV-tPA administration after the initial CTA may have changed the location of ICA occlusion sites that were confirmed on subsequent DSA. However, the low rates of recanalization with IV-tPA in acute carotid occlusion make this less of an issue. Finally, our outcome results should be carefully interpreted because our study did not include acute ICA patients who underwent currently available thrombus retrieval technology. Therefore, more detailed studies concerning the aftermath of this new technology are warranted.

5. Conclusion

In summary, our results indicate that the occlusion site is a significant predictor for the prognosis of patients with acute symptomatic ICA occlusion. Moreover, specific CTA characteristics may be useful to promptly pinpoint the actual occlusion site in the ICA, guiding clinicians' treatment decision for patients with acute ICA occlusions.

References

- [1] Bhatia R, Hill MD, Shobha N, et al. Low rates of acute recanalization with intravenous recombinant tissue plasminogen activator in ischemic stroke: real-world experience and a call for action. *Stroke* 2010;41:2254–8.
- [2] Paciaroni M, Agnelli G, Caso V, et al. Intravenous thrombolysis for acute ischemic stroke associated to extracranial internal carotid artery occlusion: the ICARO-2 study. *Cerebrovasc Dis* 2012;34:430–5.
- [3] Paciaroni M, Balucani C, Agnelli G, et al. Systemic thrombolysis in patients with acute ischemic stroke and internal carotid artery occlusion: the ICARO study. *Stroke* 2012;43:125–30.
- [4] Papanagiotou P, Roth C, Walter S, et al. Carotid artery stenting in acute stroke. *J Am Coll Cardiol* 2011;58:2363–9.
- [5] Saqur M, Uchino K, Demchuk AM, et al. Site of arterial occlusion identified by transcranial Doppler predicts the response to intravenous thrombolysis for stroke. *Stroke* 2007;38:948–54.
- [6] Berkhemer OA, Fransen PS, Beumer D, et al. Endovascular therapy for ischemic stroke. *N Engl J Med* 2015;372:2363–6.
- [7] Goyal M, Demchuk AM, Menon BK, et al. A randomized trial of intraarterial treatment for acute ischemic stroke. *N Engl J Med* 2015;372:11–20.
- [8] Campbell BC, Mitchell PJ, Kleinig TJ, et al. Endovascular therapy for ischemic stroke with perfusion-imaging selection. *N Engl J Med* 2015;372:1009–18.
- [9] Saver JL, Goyal M, Bonafe A, et al. Stent-retriever thrombectomy after intravenous t-PA vs. t-PA alone in stroke. *N Engl J Med* 2015;372:2285–95.
- [10] Jovin TG, Chamorro A, Cobo E, et al. Thrombectomy within 8 hours after symptom onset in ischemic stroke. *N Engl J Med* 2015;372:2296–306.
- [11] Ringelstein EB, Zeumer H, Angelou D. The pathogenesis of strokes from internal carotid artery occlusion. Diagnostic and therapeutical implications. *Stroke* 1983;14:867–75.
- [12] Fritz VU, Voll CL, Levien LJ. Internal carotid artery occlusion: clinical and therapeutic implications. *Stroke* 1985;16:940–4.
- [13] Urbach H, Ries F, Ostertun B, et al. Local intra-arterial fibrinolysis in thromboembolic "T" occlusions of the internal carotid artery. *Neuroradiology* 1997;39:105–10.
- [14] Kim JJ, Dillon WP, Glastonbury CM, et al. Sixty-four-section multi-detector CT angiography of carotid arteries: a systematic analysis of image quality and artifacts. *AJNR Am J Neuroradiol* 2010;31:91–9.
- [15] Marquering HA, Nederkoorn PJ, Beenen LF, et al. Carotid pseudo-occlusion on CTA in patients with acute ischemic stroke: a concerning observation. *Clin Neurol Neurosurg* 2013;115:1591–4.
- [16] Furlan A, Higashida R, Wechsler L, et al. Intra-arterial prourokinase for acute ischemic stroke. The PROACT II study: a randomized controlled trial. Prolase in acute cerebral thromboembolism. *JAMA* 1999;282:2003–11.
- [17] Zaidat OO, Yoo AJ, Khatri P, et al. Recommendations on angiographic revascularization grading standards for acute ischemic stroke: a consensus statement. *Stroke* 2013;44:2650–63.

- [18] Pessin MS, Duncan GW, Davis KR, et al. Angiographic appearance of carotid occlusion in acute stroke. *Stroke* 1980;11:485–7.
- [19] de Weert TT, Cakir H, Rozie S, et al. Intracranial internal carotid artery calcifications: association with vascular risk factors and ischemic cerebrovascular disease. *AJNR Am J Neuroradiol* 2009;30:177–84.
- [20] Liebeskind DS, Flint AC, Budzik RF, et al. Carotid I's, L's and T's: collaterals shape the outcome of intracranial carotid occlusion in acute ischemic stroke. *J Neurointerv Sug* 2015;7:402–7.
- [21] Gibo H, Lenkey C, Rhoton AL Jr. Microsurgical anatomy of the supraclinoid portion of the internal carotid artery. *J Neurosurg* 1981;55:560–74.
- [22] Hacke W, Kaste M, Fieschi C, et al. Randomised double-blind placebo-controlled trial of thrombolytic therapy with intravenous alteplase in acute ischaemic stroke (ECASS II). Second European-Australasian acute stroke study investigators. *Lancet* 1998;352:1245–51.
- [23] Ay H, Furie KL, Singhal A, et al. An evidence-based causative classification system for acute ischemic stroke. *Ann Neurol* 2005;58:688–97.
- [24] Momjian-Mayor I, Baron JC. The pathophysiology of watershed infarction in internal carotid artery disease: review of cerebral perfusion studies. *Stroke* 2005;36:567–77.
- [25] Barnett HJ, Gunton RW, Eliasziw M, et al. Causes and severity of ischemic stroke in patients with internal carotid artery stenosis. *JAMA* 2000;283:1429–36.
- [26] Endo S, Kuwayama N, Hirashima Y, et al. Results of urgent thrombolysis in patients with major stroke and atherothrombotic occlusion of the cervical internal carotid artery. *AJNR Am J Neuroradiol* 1998;19:1169–75.
- [27] Lee JS, Hong JM, Kim EJ, et al. Comparison of the incidence of parenchymal hematoma and poor outcome in patients with carotid terminus occlusion treated with intra-arterial urokinase alone or with combined IV rtPA and intra-arterial urokinase. *AJNR Am J Neuroradiol* 2012;33:175–9.
- [28] Hademenos GJ, Massoud TF. Biophysical mechanisms of stroke. *Stroke* 1997;28:2067–77.
- [29] Rodrigues FB, Neves JB, Caldeira D, et al. Endovascular treatment versus medical care alone for ischaemic stroke: systematic review and meta-analysis. *BMJ* 2016;33:i1754.
- [30] Bos D, Ikram MA, Elias-Smale SE, et al. Calcification in major vessel beds relates to vascular brain disease. *Arterioscler Thromb Vasc Biol* 2011;31:2331–7.